Prace Naukowe Instytutu Maszyn, Napędów i Pomiarów Elektrycznych
Nr 69 Politechniki Wrocławskiej Nr 69

Studia i Materiały Nr 33 2013

distortion, efficiency, induction motor,
power factor, unbalance

Petr ORSÁG*, Stanislav KOCMAN*

THE INFLUENCE OF THE VOLTAGE UNBALANCE AND VOLTAGE VARIATIONS ON OPERATION CHARACTERISTICS OF AN ELECTRICAL DRIVE WITH AN INDUCTION MOTOR

Induction motors are the most widespread types of electrical motors in electrical drives. Their main advantages include high reliability, simple construction and corresponding nearly maintenance-free, and the possibility to feed them from the common AC power network. To control their speed, frequency converters are widely used in structures of adjustable speed drives. This paper deals with the influence of voltage unbalance and voltage variations in the supply network on operation characteristics of a tested adjustable speed drive with an induction motor and a frequency converter. Supply voltage parameters were adjusted using a programmable power source Pacific 3120AMX. Monitored drive parameters were computed from measured signals and depicted in graphs. Calculated parameter dependencies have confirmed an increase in the input current drive distortion and changes in its harmonic spectrum caused by an unbalance of the supply voltage, and only moderate influence of voltage variations on efficiency of drive components and total drive efficiency.

1. INTRODUCTION

Three-phase squirrel cage asynchronous motors are widely used in electrical drives, both non-adjustable and adjustable. Their large scale using and operation in various applications is given by their simple construction, reliability, low maintenance and relatively low cost. However, there is only one efficient method for controlling the induction motor speed–change of its operating frequency realized using frequency converters implemented into structures of electrical drives. These adjustable speed drives with induction motors and frequency converters are used in almost all technical applications where the speed control is required. In most cases, indirect

* VŠB-Technical University of Ostrava, FEECS, Dept. of Electrical Engineering, 17. listopadu 15, 70833 Ostrava-Poruba, Czech Republic.

frequency converters are used consisting of an uncontrolled input rectifier (diode-bridge) for the AC-DC conversion, voltage DC link (filter capacitor) and a three-phase inverter (transistor-bridge) for the DC-AC conversion. Modern frequency converters make it possible to connect with control systems, and in this way to include such drives in an automated system. Apart from a number of significant advantages, the use of frequency converters also has some disadvantages. These include higher costs, drive complexity, negative influences on some motor parameters and problems related to electromagnetic compatibility [1]. Frequency converters draw significantly non-harmonic current from the network, and they are a source of high frequency disturbances [2]–[4].

In the case that the input rectifier of a frequency converter is three phase fed, the harmonic spectrum of drawn current includes elements that are typical for the three-phase rectifier, i.e., 1st, 5th, 7th, 11th, etc., all of these being odd harmonics, excluding multiples of three [3]. In the case of unbalanced supply voltage, harmonic currents of multiples of three are also included in the drawn current harmonic spectrum.

Unbalance in three-phase systems is classified by a coefficient of voltage unbalance. It is defined as negative sequence component divided by positive sequence component:

$$\rho = \left| \frac{\underline{V}_2}{\underline{V}_1} \right| \cdot 100\,(\%)\,. \tag{1}$$

The other definition is from the NEMA standard and from standard [5] using the approximate formula:

$$\rho = \max_{\mathrm{i}} \frac{V_i - V_{\mathrm{avg}}}{V_{\mathrm{avg}}} \cdot 100\,(\%)\,, \tag{2}$$

which is the maximum deviation from mean of three phase voltages divided by this mean.

Under normal working conditions, over a week's interval, 95% of all 10-minute average ρ, have to be 0 to 2%, according to ČSN-EN 50160.

Load changes cause variations of voltage in power network. Standard ČSN-EN 50160 determines that supply voltage variations should be lower than ±10% for 95% of 10-minute averages within a weekly period and +10/–15% for all 10-minute averages within a weekly period [6].

2. TESTED ELECTRICAL DRIVE

The tested electrical drive was fed by programmable power source Pacific 3120AMX, a three-phase arbitrary waveform generator, which can generate any wave-

form, with output power up to 12 kW. Output frequency range is 20–5000 Hz and output voltage distortion is 0.1% (for frequencies 20–1000 Hz) [7].

Between this programmable power source and the tested induction motor is connected frequency converter using input standard six-pulse diode bridge rectifier. No additional input or output filtering is used in the structure.

Measured circuit is shown in Fig. 1.

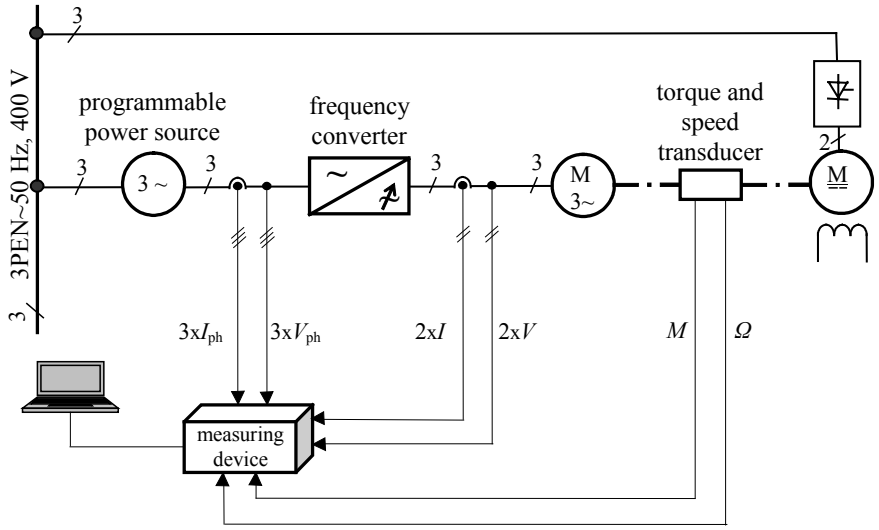

Fig. 1. Block diagram of the tested drive

Tested induction motor was three-phase squirrel cage motor Siemens 1LE10011BB634AF4 with parameters given in table 1.

Table 1. Parameters of the tested induction motor

rated power	5.5 kW	nominal speed	1460 rpm
nominal voltage	400 V	nominal efficiency	87.7%
nominal current	11.2 A	nom. power factor	0.81
nominal frequency	50 Hz	efficiency class	IE2

Torque and speed of the induction motor are measured by a HBM T20WN50 transducer. This transducer measures static and dynamic torque and rotation speed or angle of rotation. Nominal torque range is 0–50 N·m, output voltage for full range is 10 V, accuracy class 0.2%. Speed measurement is accomplished by a built in incremental sensor with 360 pulses per rotation [8].

To break the induction motor, a separately excited DC motor fed by an AC/DC converter is used.

3. DESCRIPTION OF MEASURING DEVICE

The digitized voltage, current, torque and speed signals depicted in Fig. 1 were acquired by a digital multi-channel measurement system with a sampling rate of 156.25 kSa/s and their characteristic parameters were calculated offline on a computer. Bandwidths of all measured signals were limited by signal conditioning modules to 30 kHz. The system is based on two parallel working National Instruments DAQ boards NI PCI-MIO16-E1, synchronized by the RTSI bus. Three input and two output voltages of the frequency converter were recorded by the first board. Corresponding current signals and both torque and speed were recorded by the second board. Five isolation modules DAQP-HV-B were used for signal conditioning of the first board and seven isolation modules DAQP-LV-BNC were used for signal conditioning of the second board. All isolation modules, manufactured by Dewetron, are equipped with high precision signal conditioning amplifiers. The transducer LEM LA 25 NP was used for the measurement of all currents. As mentioned above, torque and speed signals were obtained by the transducer HBM T20WN50.

4. FORMULAS FOR CALCULATION OF SELECTED CHARACTERISTIC PARAMETERS OF MEASURED SIGNALS

The total input current harmonic distortion of the frequency converter was computed from the following formula:

$$THD_I = \frac{1}{J}\sum_{j=1}^{j=J} THD_{I_j} = \frac{1}{J}\sum_{j=1}^{j=J} \frac{\sqrt{\sum_{h=2}^{h=40} I_{j(\mathrm{h})}^{\,2}}}{I_{j_{(1)}}} \tag{3}$$

where:

- j – the index of the consecutive period of a signal,
- J – the integer number of its periods,
- h – order of harmonic components of the signal spectra,
- $I_{j(h)}$ – the rms value of the h-th harmonic current component computed into the j-th period of the current signal.

Similarly, motor power factor was computed from the following formula [9]:

$$\cos(\varphi + 30°) = \frac{1}{J}\sum_{j=1}^{j=J} \cos(\varphi + 30°)_j = \frac{1}{J}\sum_{j=1}^{j=J} \frac{P_{\mathrm{UW}_{j(1)}}}{V_{\mathrm{UW}_{j(1)}} I_{\mathrm{U}_{j(1)}}} \tag{4}$$

where:

$$P_{\mathrm{UW}_{j(1)}} = \frac{1}{N}\sum_{n=1}^{n=N} v_{\mathrm{UW}_{(1)}}(n)\, i_{\mathrm{U}_{(1)}}(n) \tag{5}$$

is the harmonic active power of the tested motor obtained using Aron's theorem, and

$$V_{\mathrm{UW}_{j(1)}} = \frac{1}{N}\sum_{n=1}^{n=N} v_{\mathrm{UW}_{(1)}}^{2}(n), \tag{6}$$

$$I_{\mathrm{U}_{j(1)}} = \frac{1}{N}\sum_{n=1}^{n=N} i_{\mathrm{U}_{(1)}}^{2}(n), \tag{7}$$

are rms values of the fundamental motor line voltage and current components enumerated into the j-th period of both signals and N is the number of samples in one period of measured signals $v_{\mathrm{UV}}(n)$ and $i_{\mathrm{U}}(n)$.

The input active power of the drive was computed from the following formula:

$$P_{\mathrm{in}} = \frac{1}{L}\sum_{l=1}^{l=L}[v_1(l)\cdot i_1(l) + v_2(l)\cdot i_2(l) + v_3(l)\cdot i_3(l)] \tag{8}$$

which is the arithmetic means of products of the digitized instantaneous voltage and current values on the frequency converter input, where l is the index of the l-th sample both input voltage $v_i(l)$ and input current $i_i(l)$, $L = J{\cdot}N$ is the number of samples in the observation time interval and the subscript i denotes the phase sequence of the three phase system on the input side of the frequency converter.

In the same way, the motor input power was computed from Aron's formula:

$$P_{\mathrm{el}} = \frac{1}{L}\sum_{l=1}^{l=L}\{v_{\mathrm{UW}}(l)\cdot i_{\mathrm{U}}(l) + v_{\mathrm{VW}}(l)\cdot i_{\mathrm{V}}(l)\} \tag{9}$$

where:

$v_{\mathrm{UW}}(l)$, $v_{\mathrm{VW}}(l)$ – are the l-th samples of motor line voltage signals,

$i_{\mathrm{U}}(l)$, $i_{\mathrm{V}}(l)$ – are the l-th samples of motor line current signals.

Motor power was computed from this formula:

$$P_{\mathrm{m}} = \frac{1}{L}\sum_{l=1}^{l=L}[m(l)\cdot\omega(l)] \tag{10}$$

where:

$m(l)$ – the l-th sample of the motor torque signal,

$\omega(l)$ – the l-th sample of the motor angular velocity signal.

Total efficiency of the drive was computed from the following relation:

$$\eta_{\text{tot}} = \frac{P_{\text{m}}}{P_{\text{in}}} \cdot 100\,(\%)\,, \tag{11}$$

converter efficiency as:

$$\eta_{\text{c}} = \frac{P_{\text{el}}}{P_{\text{in}}} \cdot 100\,(\%)\,, \tag{12}$$

and motor efficiency as:

$$\eta_{\text{m}} = \frac{P_{\text{m}}}{P_{\text{el}}} \cdot 100\,(\%)\,. \tag{13}$$

5. EXPERIMENTAL MEASUREMENT RESULTS

First set of measurements was supposed to evaluate the influence of voltage unbalance on input current harmonics. The following figures illustrate influences of the adjusted levels of the voltage unbalance on input current distortion and its spectrum.

Figure 2 shows input voltage and current waveforms when the supply voltage was balanced with total harmonic distortion $THD_V = 0.5\%$, in Fig. 3 is corresponding input current harmonic spectrum for motor loading of 75%. The total input current harmonic distortion is $THD_I = 127\%$. Frequency adjusted to 50 Hz on the drive converter. As can be seen in Fig. 3, the dominant harmonic currents of the 5th, 7th, 11th and 13th orders reach considerable high values, whereas triple harmonics are negligible.

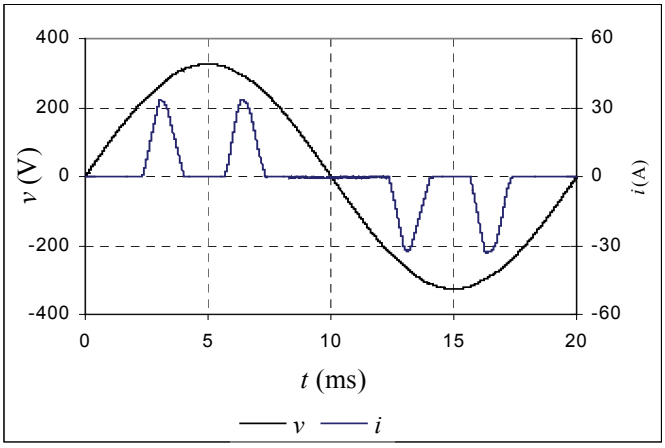

Fig. 2. Waveforms of the drive input voltage and current
(unbalance = 0%, 75% load)

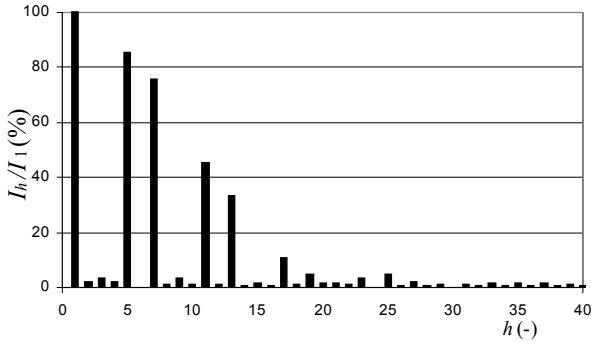

Fig. 3. Spectrum of the drive input current (unbalance = 0%, 75% load)

The total input current harmonic distortion THD_I depending on the load is shown in Fig. 4 under the adjusted levels of output frequency ranging from 30 Hz up to 70 Hz.

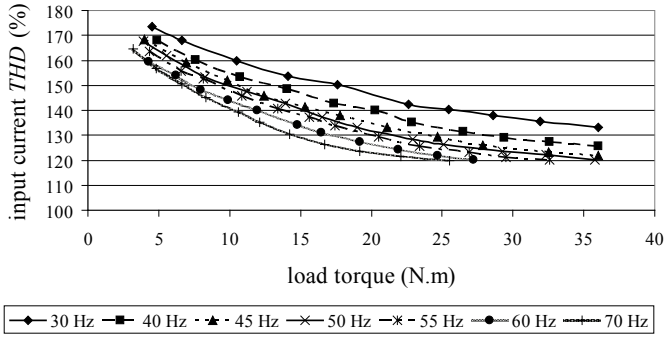

Fig. 4. Total input current harmonic distortion THD_I versus load under adjusted levels of output frequency (unbalance = 0%, THD_V = 0.5%)

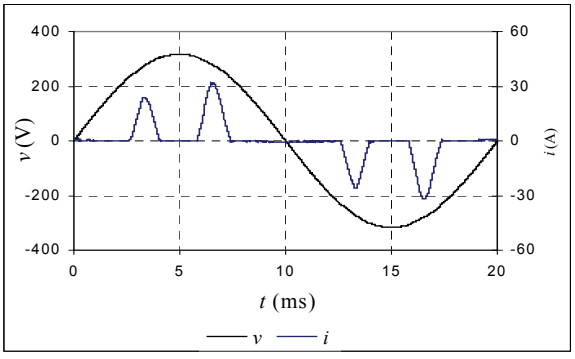

Fig. 5. Waveforms of the drive input voltage and current (unbalance = 2%, 75% load)

Consequently, input voltage and current waveforms are shown in Fig. 5 with adjusted level of the voltage unbalance to 2% on the programmable power source. As seen, the unbalance causes a change in the current waveform corresponding with a change of the input current spectrum where besides characteristic harmonics also non-characteristic triple harmonics appear as it can be seen in Fig. 6. The measurement was performed under motor load of 75%, the total input current harmonic distortion THD_I = 136%. Frequency adjusted to 50 Hz on the drive converter.

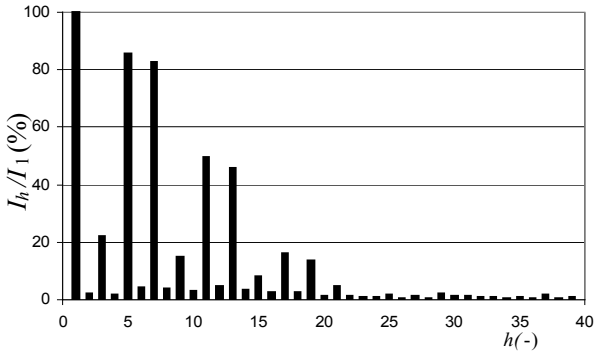

Fig. 6. Spectrum of the drive input current (unbalance = 2%, 75% load)

In Figure 7 the input current THD_I depending on the load is shown under the adjusted levels of voltage unbalance equal to 0%, 1% and 2%. All curves are for output frequency adjusted to 50 Hz, results for other tested frequencies are very similar.

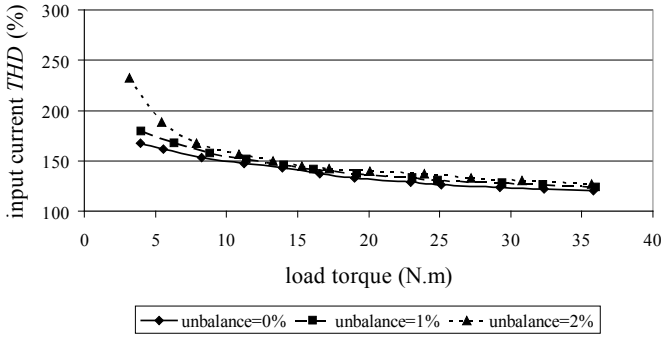

Fig. 7. Total input current harmonic distortion THD_I versus load under adjusted levels of voltage unbalance (f = 50 Hz, THD_V = 0.5%)

Motor power dependency on the motor load torque under adjusted levels of motor supply frequencies is shown in Fig. 8. These dependencies are predictably linear for all frequencies.

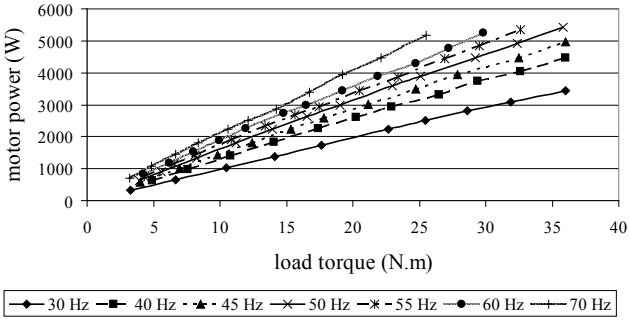

Fig. 8. Motor power versus load torque (unbalance = 0%, THD_V = 0.5%)

Motor efficiency depending on the load was also examined and it is shown in Fig. 9 under balanced and almost sinusoidal supply voltage and for adjusted levels of frequency, and in Fig. 10 under adjusted levels of voltage variations of 5% and 10% of nominal voltage, respectively.

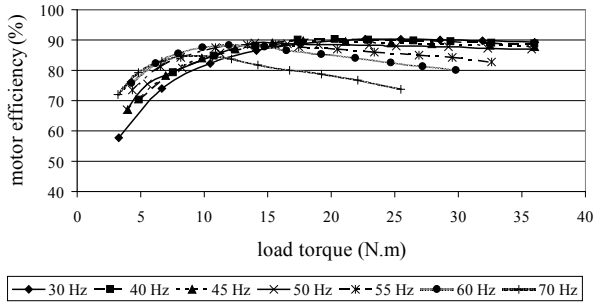

Fig. 9. Motor efficiency versus load torque under adjusted levels of output frequency (unbalance=0%, THD_V = 0.5%)

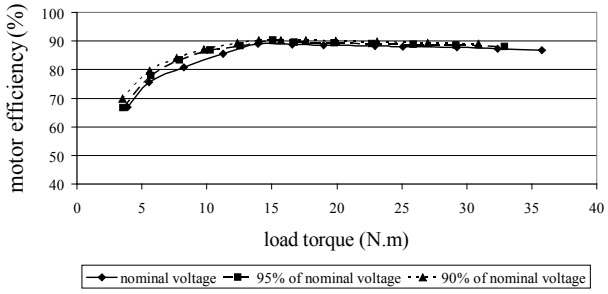

Fig. 10. Motor efficiency versus load torque under adjusted levels of voltage variations (f = 50 Hz, unbalance = 0%, THD_V = 0.5%)

In this case the converter output frequency was adjusted to the value of 50 Hz. The voltage unbalance of the adjusted levels has almost no influence on motor and converter efficiency, which is not examined under the unbalance in the following part of this paper.

As seen in Fig. 10, voltage variations in the range up to 10% of the nominal voltage have only moderate influence on the motor efficiency in the wide range of loading. Experimental measurements for other tested frequencies bring similar results.

Similarly the dependency of frequency converter efficiency on the load under adjusted levels of its output frequency is shown in Fig. 11, and in Fig. 12 under adjusted levels of voltage variations of 5% and 10% of nominal voltage, respectively.

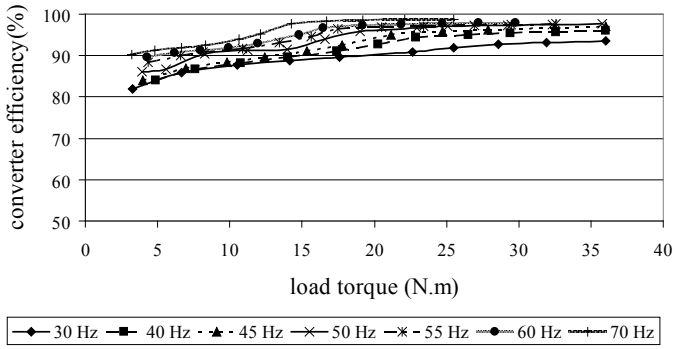

Fig. 11. Converter efficiency versus load torque under adjusted levels of output frequency (unbalance = 0%, THD_V = 0.5%)

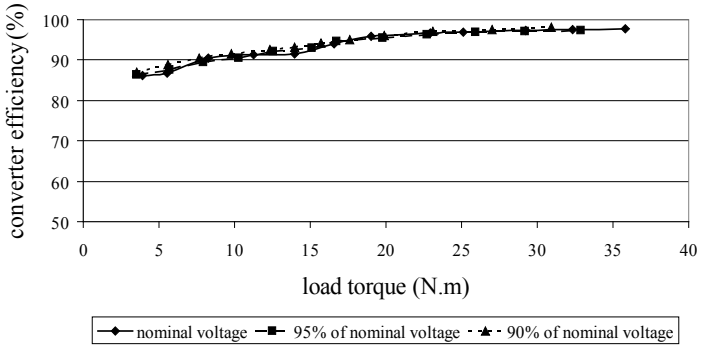

Fig. 12. Converter efficiency versus load torque under adjusted levels of voltage variations (f = 50 Hz, unbalance = 0%, THD_V = 0.5%).

Total efficiency of the drive is shown in Fig. 13, and Fig. 14, respectively. The way of presentation is the same as in the case of the above mentioned motor and converter efficiency.

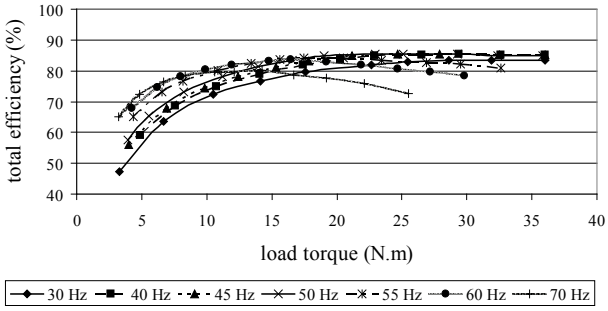

Fig. 13. Total drive efficiency versus load torque under adjusted levels of output frequency (unbalance = 0%, THD_V = 0.5%)

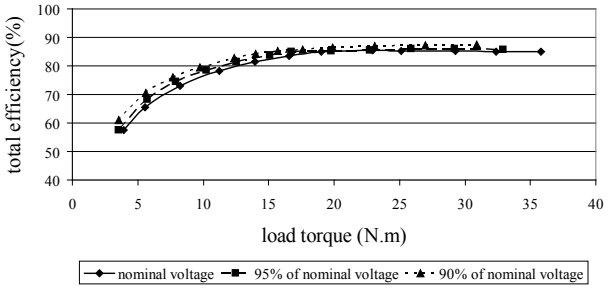

Fig. 14. Total drive efficiency versus load torque under adjusted levels of voltage variations (f = 50 Hz, unbalance = 0%, THD_V = 0.5%)

Induction motor power factor cosφ varies with motor loading and with the level of output frequency and voltage variations as seen in Fig. 15, and in Fig. 16, respectively. The adjusted frequencies above the nominal value of 50 Hz and reduced drive supply voltage increase values of motor power factor which can be observed in the both figures.

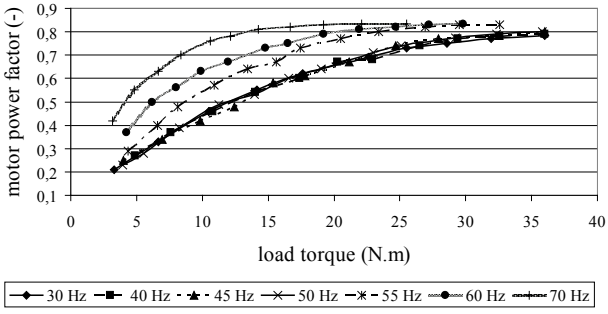

Fig. 15. Motor power factor cosφ versus load torque under adjusted levels of output frequency (unbalance = 0%, THD_V = 0.5%)

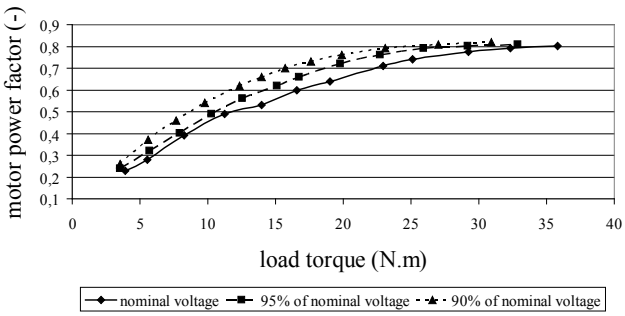

Fig. 16. Motor power factor cosφ versus load torque under adjusted levels of voltage variations (f = 50 Hz, unbalance = 0%, THD_V = 0.5%)

6. CONCLUSION

Influence of the voltage unbalance, voltage variations and the converter output frequency on characteristic energy parameters of the drive but also the total input current harmonic distortion of the drive converter in dependence on the motor load was investigated in the paper.

Experimental measurements confirmed that the standard allowable 2% voltage unbalance of supply network leads to observable asymmetric currents on the input side of the drive converter, so due to the asymmetry the third harmonic current components are injected into the supply network. However, measurements showed that the voltage unbalance has little effect on the total input current harmonic distortion.

Voltage dip measurements performed by 5% and 10% of the nominal voltage variation showed that the motor drive efficiency in contrast to the motor power factor doesn't so much depend on supply network voltage variations and there is nearly no dependence of the converter efficiency on voltage variations.

Frequency measurement showed that the total input current harmonic distortion and the converter efficiency in contrast to the total efficiency, the motor efficiency and the motor power factor don't depend on speed control method of the investigated drive (U/f = const. mode in range 30–50 Hz and P = const. mode in range 50–70 Hz) and that the total input current harmonic distortion, the converter efficiency and the motor power factor in P = const. mode strongly depend on the converter output frequency at the given motor load.

ACKNOWLEDGMENT

This work was supported in part by the Moravian-Silesian Region under Grant 02438/2009/RRC.

REFERENCES

[1] DECNER A., *The efficiency of electric drives supplied from frequency converters (PWM) and parasitical effects occurring in induction motors*, Energy Efficiency in Motor Driven Systems, Berlin, Springer-Verlag, 2003, 78–85.
[2] KOCMAN S., *EMC u regulovaných pohonů se střídavými motory*, Ph.D. thesis, VSB-Technical University of Ostrava, 2004 (in Czech).
[3] KŮS V., *Vliv polovodičových měničů na napájecí soustavu*, BEN, 2002 (in Czech).
[4] VACULÍKOVÁ P., VACULÍK E., AND ET. AL, *Elektromagnetická kompatibilita elektrotechnických systémů*, Grada, 1998 (in Czech).
[5] EN 61 000 2-1, *Electromagnetic compatibility (EMC) – Part 2-1: Environment – Description of the environment – Electromagnetic environment for low frequency conducted disturbances and signaling in public power supply systems*, ČNI, 1993 (in Czech).
[6] EN 50160, *Voltage characteristics of electricity supplied by public distribution systems*, ČNI, 2011 (in Czech).
[7] Pacific AMX Power Source manual, Pacific Power Source, Irvine, USA 2001.
[8] HBM Torque transducer operating manual, Hottinger Baldwin Messtechnik GmbH, Darmstadt, BRD.
[9] WEBSTER J.G., *Electrical measurement, signal processing, and displays*, CRC Press, 2004.